Journal of The Electrochemical Society

The Electrochemical Society
Advancing solid state & electrochemical science & technology

OPEN ACCESS

Additive Manufacturing of Microcantilevers of Varying Stiffnesses for Sensing Applications

To cite this article: Shervin Foroughi *et al* 2022 *J. Electrochem. Soc.* **169** 027507

Journal of The Electrochemical Society, 2022 **169** 027507
1945-7111/2022/169(2)/027507/5/$40.00 © 2022 The Author(s). Published on behalf of ECS by IOP Publishing Limited

Additive Manufacturing of Microcantilevers of Varying Stiffnesses for Sensing Applications

Shervin Foroughi,* Mohsen Habibi,[z] and Muthukumaran Packirisamy

Optical-Bio Microsystems Laboratory, Micro-Nano-Bio Integration Center, Mechanical, Industrial and Aerospace Engineering, Gina Cody School of Engineering and Computer Science, Concordia University, Montreal, QC H3G 1M8, Canada

Fabrication of the microcantilevers using the traditional methods is time-consuming and costly. With the advancement of additive manufacturing methods, the fabrication of functional microcantilevers is possible. This work presents the fabrication of elastomeric microcantilevers using the SLA 3D printing technology. Different microcantilevers are fabricated. The mechanical characteristics of the fabricated cantilevers are identified by performing micromechanical tests. Results show that the cantilevers' measured stiffnesses are comparable with those reported in the literature. The method explained in this work reveals the possibility of employing SLA 3D printing and soft elastomeric printing materials to fabricate microcantilevers.
 [DOI: 10.1149/1945-7111/ac50e1]

Manuscript submitted September 21, 2021; revised manuscript received January 8, 2022. Published February 10, 2022. *This paper is part of the JES Focus Issue on the 18th International Meeting on Chemical Sensors (IMCS-18) – Volume Two.*

Microcantilevers are simple structures with numerous physical, biological, and chemical sensing applications. They have been employed for the determination of the fluid viscosity and density,[1] detection of biomolecular interaction,[2] and the level of ammonia in the ambient atmosphere.[3] The silicon-based microcantilevers are the most common type of these microdevices. However, the biological and physical applications of other polymeric and polymer-composite microcantilevers have been reported in the literature.[4,5]

Microcantilevers might be in rectangular, triangular, or double-legged shapes[6] with long or short lengths in a single[7] or array[8] form. The size and stiffness of the cantilevers are the parameters that affect the deflection of the microcantilevers. Commonly, microcantilevers can operate in two modes: static and dynamic. In the dynamic operation, the cantilever's resonance frequency is the desired parameter to be measured. However, the magnitude of the structural deflection in the static operation shows information about the process.[9] The dynamic behavior of the microcantilever can be occurred by the loading caused by the mass adsorption or desorption from the medium, elasticity changes during the operation, or viscous damping of the fluid medium.[9] Asymmetric-induced surface stresses or external forces are the causes for inducing static deformation in microcantilevers.[6] Microcantilevers with low stiffness and long length can undertake large deflections, suitable for performing the static mode detections. In contrast, the cantilevers with high stiffness and short length are used for dynamic detection.[10]

The polymeric cantilevers have lower Young's modulus than those made of silicon and are more sensitive to static deflection measurement.[11] The movement of the operational cantilevers can be detected by employing common detection techniques, including piezoresistive, capacitive, and optical methods.[12] These techniques are capable of measuring the small movements of the cantilevers. Among these methods, the non-contact optical detection method is accurate enough to measure the movements in a range of nanometers to micrometers.[6]

Micromachining and lithography are two common technologies employed in fabricating microcantilevers.[10,13] Polydimethylsiloxane (PDMS) and SU-8 are common polymers used for fabricating cantilevers through the soft-lithography process. The advancements in additive manufacturing (AM) technologies showed that 3D printing has considerable potential in the fabrication of microfluidic devices without the need for soft lithography.[14,15] In the conventional 3D printing process, the three-dimensional prototypes of functional objects are fabricated from computer-generated three-dimensional (3D) geometry models in a layer-by-layer fashion. In the layer-by-layer method, the desired object is created by successively stacking up multilayers of material. Among the existing AM technologies, stereolithography (SLA) has been widely used to fabricate complex microfluidic devices.[16] Comparing the SLA with conventional soft lithography for fabrication of the microfluidic devices reveals that this method is more convenient, quicker, and cost-effective than soft lithography.[17,18] Also, SLA enables the production of 3D structures that are not conceivable with PDMS molding.[17]

Recently, SLA, inkjet 3D printing, and digital light processing (DLP) technologies were used for the fabrication of the polymeric microcantilevers,[19–21]. Credi et al.[19] employed SLA technology to build bimaterial cantilevers with the dimensions of 9 mm × 0.6 mm × 0.2 mm (length × width × thickness) to investigate the application of ferromagnetic photopolymer in the manufacturing of functional microstructures. The polymeric cantilevers can be employed in chemical, bio, and flow sensing applications,,[20,22–2420,22–24] Stassi et al.[20] used the DLP technology for building an array of polymeric microcantilevers for biosensing applications with the size of 3 mm × 0.7 mm × 0.2 mm (length × width × thickness) and elasticity modulus of 0.9 GPa. To study the usage of 3D printed microcantilevers as part of sensors or actuators, Kawa et al.[21] presented the mechanical characterization of the plastic microcantilevers using an inkjet 3D printer. Cantilevers were fabricated in different dimensions (2 mm ∼ 8 mm length, 2 mm width, and 0.2 mm ~ 0.6 mm thickness). Kawa reported the elasticity modulus of 0.28 GPa to 1.17 GPa for the fabricated microcantilevers.

The stiffness of a microcantilever affects its sensitivity[25] and may be used to compare the performance of sensors of various dimensions.[26] This parameter can vary either by increasing the aspect ratio (length/thickness) of the microcantilever or utilizing a soft structural material provided that the self-standing property of the structure is not compromised. In 3D printing of a self-standing microcantilever from a soft polymeric material, the structural aspect ratio can be reduced to improve the structure's stability while maintaining the microcantilever's sensitivity. Reducing the dimensions of the cantilever might decrease the size of the final mechanism and reduce the volume of the test samples in real applications. Therefore, in the present work, fabrication, and mechanical characterization of the soft plastic microcantilevers with different geometrical aspect ratios for being employed in sensing applications are presented.

Materials and Methods

Fabrication.—Four types of microcantilevers with different dimensions were designed using the "Solidworks" software.

*Electrochemical Society Member.
[z]E-mail: mohsen.habibi@concordia.ca

Table I. The design dimensions of microcantilevers.

Microcantilever	Dimensions (μm) Length	Width	Thickness	Aspect ratio (Length/Thickness)
Design 1	2000	300	250	8
Design 2	1500	300	250	6
Design 3	1200	300	300	4
Design 4	1000	300	300	3.3

Table I presents the dimensions of the designed cantilevers and their corresponding aspect ratios (Length/Thickness).

The CAD files were transferred in stereolithography (STL) format to the SLA 3D printer Form 2 (Formlabs Co. USA) with a resolution of 150 μm in XY directions (laser spot diameter of 150 μm) and the minimum layer thickness of 25 μm. The Flexible resin (Formlabs, USA) was used as a building material. This resin is in grey color, and the minimum layer thickness for printing by using Form 2 is 50 μm. The characteristics of the resin are presented in Table II.

Several microcantilevers have been built to find the optimized dimensions in which the self-standing property of the structure is maintained. Different printing orientations for the fabrication of the microstructures were examined. Choosing the printing orientations other than the vertical orientation requires considering the removable structural supports for the fabrication process. Although these supports will be removed upon completing the 3D printing, some spots will remain on the cantilever, which changes the beam's geometry. As a result, to avoid any extra structural supports, the microcantilevers were fabricated in a vertical orientation perpendicular to the surface of the building platform. The layer thickness of the 3D printer was set to 100 μm, and for each design category presented in Table I, four microcantilevers were 3D printed. The 3D printing of all cantilevers took 2.5 h. Upon finishing the printing, the cantilevers were detached from the platform and washed with isopropanol (IPA) to remove uncured resins and dried with air. Then, to complete the solidification process, the microcantilevers were exposed to UV light in a Stratalinker UV Crosslinker 2400 (wavelength = 254 nm, Stratagene, USA) for five minutes. Then, the cantilevers were washed in IPA to remove any remaining sticky materials from the surface of the cantilever. Figure 1 illustrates the microcantilever CAD design and 3D printed cantilevers on the building platform before and after postprocessing. The final microcantilevers were used to perform the mechanical characterization. The base supports indicated in Fig. 1 a were considered for facilitating the handling of the microcantilevers during the experiments.

Measurements.—After the preparation process, the Confocal Laser Scanning Microscope (Olympus Inc.) was used to measure the dimensions and surface roughness of the microcantilevers. The roughness was measured by scanning the area of 1 mm by 0.2 mm over the top surface of the beams. The cutoff value of 0.25 mm was set for the measurements. The dimensions and surface roughness data were gathered using the 5× and 10× lenses, respectively. Figure 2 illustrates a captured image of a 1 mm microcantilever using the confocal microscope.

Table II. Material properties of flexible resin.

Tear strength of printed object[a)]	13.3–14.1 kN m^{-1}
Ultimate tensile strength of post-cured object[a)]	7.7–8.5 MPa
Elongation at failure[a)]	75–85%
Viscosity[b)]	7.3 Pa.s

a) Based on material datasheet provided by Formlabs Co. b) Voet et al.[27]

Due to the nature of the layer-by-layer process implemented in SLA technology, the defects in sawtooth form can be observed at the surfaces of the 3D printed cantilevers, which results in the dimensional variation of the final objects. Therefore, to investigate the dimensional resolution of the fabricated microcantilevers, the depth of the notches (d) and the angles between two consecutive layers (α) were measured by using the confocal microscope as shown in Fig. 2.

The static deflection-load experiments were performed to measure the beams' linear stiffness. The experiments were done using the FemtoTools FT-MTA02 Micromechanical Testing and Assembly Station. This device is a micromechanical testing tool with a wide range of applications for biomaterials testing, micro/nanosystems characterization, and material science. This apparatus includes the micro-robotic system with nanometer manipulation resolution in XYZ, and the universal measurements stand equipped with the digital microscope. This device is equipped with the sensing probe with the needle tip section size of (50 × 50 μm), the thickness of 50 μm, force range of ±100000 μN, and resolution of 5 μN, which is being mounted on a micro-robotic system. This probe was used for the tests. The experiments were carried out by continuously applying a maximum deflection of 300 μm (about 1/3 of the length of the shortest cantilever) at a distance of ∼100 μm with the tip of the cantilever. Limiting the maximum deflection of the microcantilever prevented the probe from sliding over the beam's surface. The probe measured the corresponding resistive force exerted by the beam, which was continuously recorded by the software dedicated to the system. The measurement process was performed three times for each microcantilever. Figure 3 shows the sensing probe in contact with a cantilever at the beginning of the measurement process.

In order to estimate Young's modulus of the fabricated microcantilevers, the following formula, which is applicable for the Eulerian beams, will be used. Generally, this equation calculates the maximum deflection at the free end of the beam due to the applied point load at that location.

$$\delta_B = \frac{PL^3}{3EI} \quad [1]$$

where δ_B is the maximum deflection at the free-end (m), P stands for the magnitude of the point load exerted at the free-end (N), L is the length of the microcantilever (m), E denotes Young's modulus (Pa), and I is the moment of inertia (m^4).

Results

Table III presents the average dimensions of the fabricated microcantilevers shown in Fig. 1c, measured using the confocal microscope.

The average measured surface roughness of the microcantilevers is presented in Table IV. The results were obtained by the fine scanning of area (1 mm by 0.2 mm) over the surface of the fabricated cantilevers.

Microcantilevers structure investigation using confocal microscope determined the variation of the angles and the notches depth in a range of 80.12°∼ 142.6° and 3.62 μm ∼ 29.83 μm, respectively.

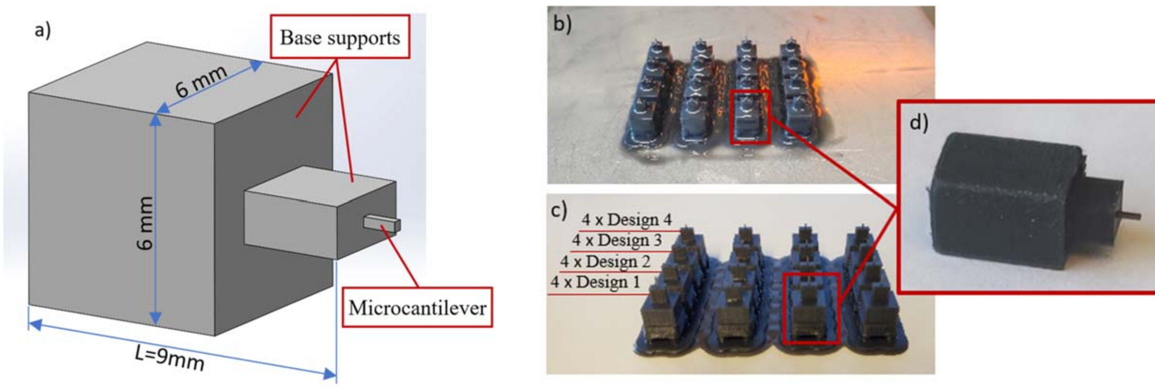

Figure 1. (a) Cad design of the microcantilever (b) Four sets of fabricated microcantilevers on a building platform of SLA 3D printer before wash (c) The microcantilevers after postprocessing being used for performing mechanical characterization experiments (d) An individual microcantilever.

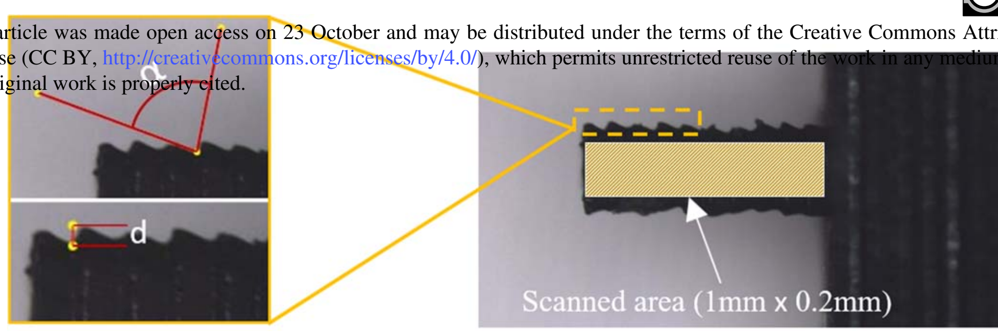

Figure 2. Identifying the scanned area for a surface roughness measurement, the notch depth, and angle between two consecutive layers using confocal microscopy (5× lens) for the microcantilever Design 4.

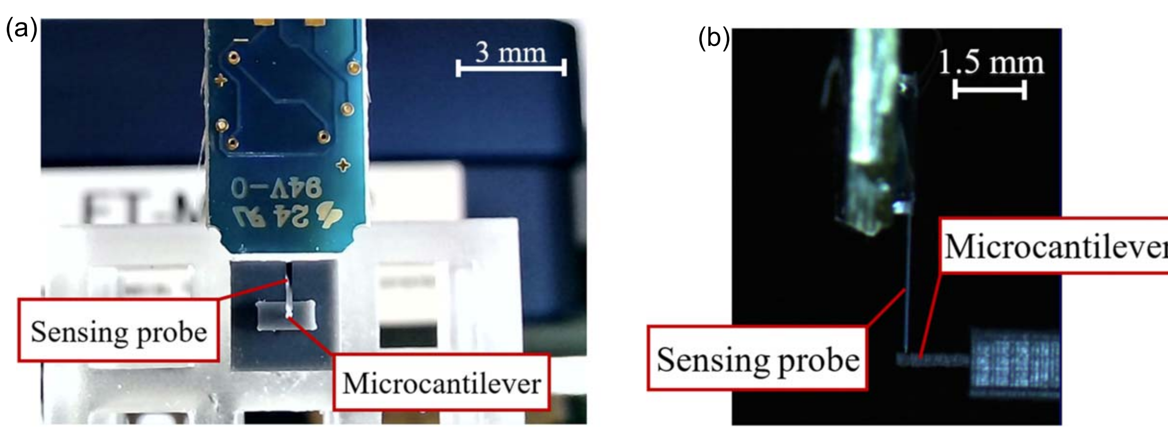

Figure 3. The (a) front view and (b) side view of the sensing probe needle in contact with the tip of the microcantilever.

Table III. Measured dimensions of 3D printed microcantilevers.

	Dimensions (μm)		
Microcantilever	Length (±18.3)	Width (±32.3)	Thickness (±29.6)
Design 1	2000	300	250
Design 2	1500	300	250
Design 3	1200	300	300
Design 4	1000	300	300

The force-deflection experimental results for the microcantilevers with different geometrical aspect ratios are shown in Fig. 4.

The trend of graphs shows that each graph can be divided into two semi-linear parts extended between [0 μm ∼ 80 μm] and [80 μm ∼ 300 μm]. The slope of each separated graph presents the stiffness of microcantilevers with respect to the range of applied displacements. Table V shows the stiffnesses of the microcantilevers for each segment.

Table IV. The measured surface roughness of the microcantilevers.

Microcantilever	Average surface roughness (μm)
Design 1	9.56
Design 2	10.04
Design 3	9.88
Design 4	11.573

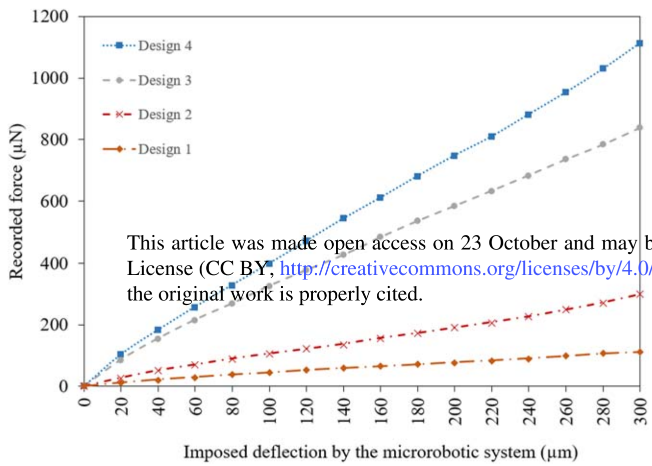

Figure 4. Induced force due to applied deflections at the tip of microcantilevers.

microcantilevers were fabricated in a layer-by-layer process by stacking up the 100 μm layers along the object's length. The Form 2 printing process includes frequent movements of the resin tank and building platform in horizontal and vertical directions. Due to the cantilevers' small dimensions, the resin's high viscosity, and flexibility of solidified material, the movements cause slight deviations of the beams from its axis and non-uniform stacking up of the consecutive layers and formation of the sawtooth defects over the surface of the beams. However, this effect is less prominent while printing the rigid microcantilevers from the corresponding resin (ex., Clear resin). The sawtooth surface defects influence the printed microcantilevers' dimensional resolution and produce non-uniformity in the cross-sectional areas of the beams along their length. Results show that the surface roughness is independent of the geometrical dimensions of the microcantilevers. Therefore, either the resolution of the 3D printer or movements during the printing process might affect the dimensional accuracy and the surface roughness of the beams. However, for futu[illegible]tion on the performance of the microcantilevers and ch[illegible]r coating or read-out methods, the other accurate surface roughness measurement methods, such as fractal-based statistical measurement, can be carried out.[28,29]

Investigation of the Force-Deflection experiments' results reveals the bilinear response of the cantilevers, as illustrated in Fig. 3, due to the tiny deflection imparted on all microcantilevers irrespective of their size. In addition, variation of the cross-sectional areas along the length of cantilevers and the eccentricity of the neutral axis might also affect the cantilever's structural behavior. The microcantilevers react stiffer in the presence of the low deflections. When the samples deflect beyond 80 μm, the linear relationship between force and deflection may be seen.

Table V. The stiffness of the microcantilevers calculated from graphs presented in Fig. 3.

Microcantilever	Stiffness ($\frac{N}{m}$)	
	Deflection [0 μm $\sim$ 80 μm]	Deflection [80 μm $\sim$ 300 μm]
Design 1	0.47	0.33
Design 2	1.11	0.92
Design 3	3.34	2.56
Design 4	4.07	3.50

The calculated stiffnesses show the direct relation between the microcantilever's sensitivity and its geometrical aspect ratio.

Table VI indicates the calculated elasticity modulus of the microcantilevers for the loads generated at the deflections of 80 μm and 300 μm, presented in Fig. 4.

These results were obtained based on the linear elastic beam theory, which estimates the elasticity modulus roughly. These results can further be verified by performing experiments such as standard tensile tests.

Discussions

The 3D printer's resolution is the parameter that significantly affects the geometrical accuracy of the printed object. The presented

Results show that the stiffness of the cantilevers is affected by their geometrical aspect ratio. The low mechanical stiffnesses of Design 1 and 2 are comparable with the cantilever's stiffness $\left(k = 0.46\frac{N}{m}\right)$ made from polydimethylsiloxane (PDMS) through the soft lithography method reported by Nezhad et al.[24] In addition, Young's modulus of the microcantilevers presented in Table VI is comparable with the elasticity modulus of the 3D printed cantilevers reported by Stassi[20] (0.9Gpa) and Kawa[21] (0.28 GPa to 1.17 GPa). This achievement justifies the approach used in this work to fabricate the microcantilevers.

Table VI. The calculated Young's modulus of the microcantilevers for the loads and deflections presented in the graphs of Fig. 3.

Microcantilever	Young's modulus (GPa)	
	Maximum deflection at 80 μm	Maximum deflection at 300 μm
Design 1	3.26	2.53
Design 2	3.23	2.86
Design 3	2.87	2.38
Design 4	2.03	1.83

Conclusions

This study reports additive manufacturing of the polymeric microcantilevers with different dimensions using SLA 3D printing technology for micro-sensing applications. The desktop SLA 3D printer "Form 2" was used to build multiple microcantilevers with different sizes. The microcantilevers' mechanical characterization was done by performing the stiffness and surface roughness measurements. The experimental results of stiffness were comparable with the polymeric microcantilever made of PDMS reported in the literature. This work reveals the possibility of fabricating functional microcantilevers using the commercial SLA 3D printers. Although this study presented the mechanical characteristics of the polymeric flexible microcantilevers, employing different light-based AM technologies and soft polymeric materials to fabricate the microcantilevers, as well as further investigations on the performance of the microcantilevers such as mass absorption for the specific applications, pave the way for future research on additive manufacturing of polymeric microcantilevers with variety of desired mechanical properties at low cost and reasonable fabrication time.

Acknowledgments

S.F. acknowledges the Fonds de Recherche du Québec – Nature et Technologies (FRQNT) for the doctoral scholarships.

ORCID

Mohsen Habibi https://orcid.org/0000-0002-3793-454X
Muthukumaran Packirisamy https://orcid.org/0000-0002-1769-6986

References

1. D. Kim, S. Hong, J. Jang, and J. Park, "Determination of fluid density and viscosity by analyzing flexural wave propagations on the vibrating micro-cantilever." *Sensors*, **17**, 1 (2017).
2. J. Amritsar, S. Foroughi, D. Raju, S. Pakkiriswami, and M. Packirisamy, "Conformational detection of heat shock protein through bio-interactions with microstructures." *Research on Biomedical Engineering*, **36**, 89 (2020).
3. M. Liu, S. Guo, P. Xu, H. Yu, T. Xu, S. Zhang, and X. Li, "Revealing humidity-enhanced NH3 sensing effect by using resonant microcantilever." *Sensors and Actuators B: Chemical*, **257**, 488 (2018).
4. V. Seena, A. Rajorya, P. Pant, S. Mukherji, and V. R. Rao, "Polymer microcantilever biochemical sensors with integrated polymer composites for electrical detection." *Solid State Sciences*, **11**1606 (2009).
5. H. Sadabadi and M. Packirisamy, "Nano-integrated suspended polymeric microfluidics (SPMF) platform for ultra-sensitive bio-molecular recognition of bovine growth hormones." *Scientific reports*, **7**, 1 (2017).
6. S. K. Vashist, "A review of microcantilevers for sensing applications." *J. of Nanotechnology*, **3**, 1 (2007).
7. R. I. Hermans, B. Dueck, J. W. Ndieyira, R. A. McKendry, and G. V, "Optical diffraction for measurements of nano-mechanical bending." *Scientific reports*, **6**, 1 (2016).
8. I. S. Amiri and S. Addanki, "Simulation fabrication and characterization of microcantilever array based ozone sensor." *Results in Physics*, **10**, 923 (2018).
9. M. Sepaniak, P. Datskos, N. Lavrik, and C. Tipple, "Microcantilever transducers: a new approach in sensor technology." *Anal. Chem.*, **74**, 568A (2002).
10. J. Xu, M. V, H. S. Wasisto, and E. Peiner, "Piezoresistive microcantilevers for humidity sensing." *J. Micromechanics Microengineering*, **29**, 1 (2019).
11. M. Alvarez, K. Zinoviev, M. Moreno, and L. M. Lechuga, "Cantilever biosensors." *Optical Biosensors: Today and Tomorrow (2nd Edition)*, ed. F. S. Ligler and C. R. Taitt (Elsevier Science, Washington, DC, USA) (2008).
12. A. K. Basu, A. Basu, and S. Bhattacharya, "Micro/nano fabricated cantilever based biosensor platform: A review and recent progress." *Enzyme and Microbial Technology*, **139**, 1 (2020).
13. A. Rammohan, P. K. Dwivedi, R. Martinez-Duarte, H. Katepalli, M. J. Madou, and A. Sharma, "One-step maskless grayscale lithography for the fabrication of 3-dimensional structures in SU-8." *Sensors and Actuators B: Chemical*, **153**, 125 (2011).
14. A. V. Nielsen, M. J. Beauchamp, G. P. Nordin, and A. T. Woolley, "3D printed microfluidics." *Annual Review of Analytical Chemistry*, **13**, 45 (2020).
15. R. Su, J. Wen, Q. Su, M. S. Wiederoder, S. J. Koester, J. R. Uzarski, and M. C. McAlpine, "3D printed self-supporting elastomeric structures for multifunctional microfluidics." *Science advances*, **6**, eabc9846 (2020).
16. B. Carnero, C. Bao-Varela, A. I. Gómez-Varela, E. Álvarez, and M. T. Flores-Arias, "Microfluidic devices manufacturing with a stereolithographic printer for biological applications." *Materials Science and Eng* [illegible], 1 (2021).
17. A. K. Au, W. Lee, and A. Folch, "Mail-order [illegible] evaluation of stereolithography for the production of microfluidic devices." *Lab on a Chip*, **14**, 1294 (2014).
18. N. Bhattacharjee, A. Urrios, S. Kang, and A. Folch, "The upcoming 3D-printing revolution in microfluidics." *Lab on a Chip*, **16**, 1720 (2016).
19. C. Credi, A. Fiorese, M. Tironi, R. Bernasconi, L. Magagnin, M. Levi, and S. Turri, "3D printing of cantilever-type microstructures by stereolithography of ferromagnetic photopolymers." *ACS Appl. Mater. Interfaces*, **8**, 26332 (2016).
20. S. Stassi, E. Fantino, R. Calmo, A. Chiappone, M. Gillono, D. Scaiola, C. F. Pirri, C. Ricciardi, A. Chiadò, and I. Roppolo, "Polymeric 3D printed functional microcantilevers for biosensing applications." *ACS applied materials & interfaces*, **9**, 19193 (2017).
21. B. Kawa, K. Adamski, D. Lizanets, and R. Walczak, "Mechanical characterization of inkjet 3D printed microcantilevers." *Proc. XV Int. Sci. Conf. Optoelectron. Electron. Sensors COE*, p. 19 (2018).
22. A. W. McFarland and J. S. Colton, "Chemicalsensing with micromolded plastic microcantilevers." *Journal of microelectromechanical systems*, **14**, 1375 (2005) .
23. V. Seena, N. S. Kale, S. Nag, M. Joshi, S. Mukherji, and V. R. Rao, "Development a polymeric microcantilever platform technology for biosensing applications." *International Conference on Smart Materials Structures and Systems*, pp. 24-32 (2008).
24. A. S. Nezhad, M. Ghanbari, C. G. Agudelo, M. Packirisamy, R. B. Bhat, and A. Geitmann, "PDMS microcantilever-based flow sensor integration for lab-on-a-chip." *IEEE Sens. J.*, **13**, 601 (2013).
25. D. Rotake, A. Darji, and N. Kale, "Fabrication, calibration, and preliminary testing of microcantilever-based piezoresistive sensor for BioMEMS applications." *IET Nanobiotechnology*, **14**, 357 (2020).
26. D. R. Rotake and A. D. Darji, "Development a polymeric microcantilever platform technology for biosensing applications." *2018 IEEE sensors*, pp. 1-4 (2018).
27. V. S. Voet, T. Strating, G. H. Schnelting, P. Dijkstra, M. Tietema, J. Xu, A. J. Woortman, K. Loos, J. Jager, and R. Folkersma, "Biobased acrylate photocurable resin formulation for stereolithography 3D printing." *ACS omega*, **3**, 1403 (2018).
28. T. Pravinraj and R. Patrikar, "Modeling and characterization of surface roughness effect on fluid flow in a polydimethylsiloxane microchannel using a fractal based lattice Boltzmann method." *AIP Advances*, **8**, 065112 (2018).
29. R. M. Patrikar, "Modeling and simulation of surface roughness." *Applied Surface Science*, **228**, 213 (2004).